THE JOURNAL OF BIOLOGICAL CHEMISTRY VOL. 286, NO. 48, pp. 41736–41744, December 2, 2011

Heparan Sulfate Is Essential for High Mobility Group Protein 1 (HMGB1) Signaling by the Receptor for Advanced Glycation End Products (RAGE)*[S]

Received for publication, August 31, 2011, and in revised form, October 2, 2011 Published, JBC Papers in Press, October 11, 2011, DOI 10.1074/jbc.M111.299685

Ding Xu[1], **Jeffrey Young, Danyin Song, and Jeffrey D. Esko**[2]

From the Department of Cellular and Molecular Medicine, Glycobiology Research and Training Center, University of California at San Diego, La Jolla, California 92093-0687

Background: The cytokine function of the danger-associated molecular pattern protein HMGB1 is mediated through RAGE.

Results: HMGB1-RAGE signaling depends on heparan sulfate, but heparan sulfate binding to HMGB1 is dispensable.

Conclusion: Heparan sulfate is essential for HMGB1 signaling because RAGE binds heparan sulfate.

Significance: Perturbing heparan sulfate may be a novel strategy to alter RAGE-dependent signaling.

In a proteomic search for heparan sulfate-binding proteins on monocytes, we identified HMGB1 (high mobility group protein B1). The extracellular role of HMGB1 as a cytokine has been studied intensively and shown to be important as a danger-associated molecular pattern protein. Here, we report that the activity of HMGB1 depends on heparan sulfate. Binding and competition studies demonstrate that HMGB1 interacts with CHO and endothelial cell heparan sulfate. By site-directed mutagenesis, we identified a loop region that connects the A-box and B-box domains of HMGB1 as responsible for heparan sulfate binding. HMGB1-induced Erk1/2 and p38 phosphorylation is abolished when endothelial heparan sulfate is removed or blocked pharmacologically, resulting in decreased HMGB1-induced endothelial sprouting. However, mutated HMGB1 that lacks the heparan sulfate-binding site retained its signaling activity. We show the major receptor for HMGB1, receptor for advanced glycation end products (RAGE), also binds to heparan sulfate and that RAGE and heparan sulfate forms a complex. Our data establishes that the functional receptor for HMGB1 consists of a complex of RAGE and cell surface heparan sulfate.

HMGB1 (high mobility group protein B1) is an abundant DNA-binding protein that normally resides in the nucleus (1). However, inflammatory cells such as monocytes and macrophages can secrete HMGB1 actively through a non-classical, vesicle-mediated secretory pathway (2). During tissue injury, necrotic cells also release HMGB1 as a danger-associated molecular pattern protein (DAMP)[3] (3, 4). Extracellular HMGB1 behaves much like a cytokine. It stimulates inflammatory responses in many types of cells, including monocytes, macrophages, neutrophils, dendritic cells, astrocytes, and endothelial cells (1, 4–6), and induces cell migration (4, 5, 7). Much interest exists in developing ways to block HMGB1 function in the context of various diseases such as sepsis, ischemic injury, arthritis, atherosclerosis, and cancer (4, 5, 8).

HMGB1 binds to the receptor for advanced glycation end products (RAGE), a transmembrane protein with three IgG-like extracellular domains and a short cytoplasmic domain. RAGE is expressed at high level in alveolar epithelial cells as well as leukocytes, endothelial cells, neurons, and tumor cells (9). It binds to HMGB1 as well as other ligands, including S100 proteins, AGEs, and amyloids, through its two N-terminal IgG-like domains (9, 10). The extracellular domain of RAGE can be shed by proteolysis, yielding what is commonly referred to as soluble RAGE, or sRAGE. Alternative splicing can give rise to a soluble form of the receptor as well (9, 10). The cytoplasmic domain of RAGE lacks intrinsic kinase activity, suggesting that signal transduction upon ligand binding involves recruitment of a signaling kinase or a kinase scaffolding protein (11, 12). The inflammatory response and migration of target cells mediated by HMGB1-RAGE involve activation of MAPKs, such as Erk1/2 and p38, and NF-κB nuclear translocation (8, 9).

Both HMGB1 and RAGE have been reported to bind heparin, a property that can be exploited for protein purification. In this report, we show that HMGB1 and RAGE also bind to heparan sulfate. We mapped the heparin-binding site on HMGB1 by mutagenesis and created a mutant that lacks the capacity to bind heparan sulfate. Surprisingly, mutant HMGB1 signals normally, but its action still depends on cell surface heparan sulfate. This finding led to the discovery that RAGE is also a heparan sulfate binding protein whose activity depends on binding to cell surface proteoglycans.

* This work was supported, in whole or in part, by National Institutes of Health Grant HL57345 (to J. D. E.). This work was also supported by Postdoctoral Fellowship 0825274F from the American Heart Association (to D. X.).

[S] The on-line version of this article (available at http://www.jbc.org) contains supplemental Table S1 and Figs. S1–S3.

[1] To whom correspondence may be addressed: Dept. of Cellular and Molecular Medicine, Glycobiology Research and Training Center, University of California, San Diego, 9500 Gilman Dr., La Jolla, CA 92093-0687. Tel.: 858-822-1102; Fax: 858-534-5611; E-mail: dxu@ucsd.edu.

[2] To whom correspondence may be addressed: Dept. of Cellular and Molecular Medicine, Glycobiology Research and Training Center, University of California, San Diego, 9500 Gilman Dr., La Jolla, CA 92093-0687. Tel.: 858-822-1100; Fax: 858-534-5611; E-mail: jesko@ucsd.edu.

[3] The abbreviations used are: DAMP, danger-associated molecular pattern protein; RAGE, the receptor for advanced glycation end products; RFU, relative fluorescence units; sRAGE, soluble RAGE; HMVEC-c, human cardiac microvascular endothelial cells.

EXPERIMENTAL PROCEDURES

Proteomic Screening—U937 cells (2×10^8) were biotinylated with 0.6 mM sulfo-NHS-SS-biotin (Pierce) in 10 ml of PBS, pH 8, at 4 °C for 1 h. The reaction was stopped by adding Tris base to a final concentration of 50 mM. After two washes with cold PBS, cells were resuspended in 3 ml of ice-cold hypotonic buffer (10 mM Tris, 10 mM NaCl, 1.5 mM $MgCl_2$, pH 7.4) supplemented with protease inhibitors. Cells were next subjected to 20 strokes in a Dounce homogenizer and then centrifuged at $1000 \times g$ for 3 min to remove intact nuclei and unbroken cells. The post-nuclear supernatant was solubilized with Nonidet P-40 (final concentration of 1%)in 150 mM NaCl and clarified by centrifugation at $14,000 \times g$ for 15 min.

U937 supernatant (~ 10 mg of protein) was diluted to 1 mg/ml with heparin column wash buffer (20 mM HEPES, 150 mM NaCl, 1% Nonidet P-40, pH 7) and applied to a heparin fast flow Sepharose column (1 ml; GE Healthcare). The column was washed with 10 ml of wash buffer and eluted sequentially with 5 ml of buffer containing 300 mM NaCl, 3 ml of 500 mM NaCl and 3 ml of 1 M NaCl. The 500 mM and 1 M eluates were combined (~1 mg of protein).

The sample was mixed with 100 μl of neutravidin beads (Pierce) in a 2-ml disposable column (Bio-Rad) and incubated at room temperature for 30 min with gentle rotation. Once the beads settled, the column was washed twice with 1 ml of cold wash buffer (1% Nonidet P-40, 0.1% SDS in PBS), twice with 1 ml of cold 1 M KCl, and twice with 1 ml of 0.1 M Na_2CO_3, pH 11.5. The beads were next washed with 3 ml of PBS and transferred into a 1.5-ml centrifuge tube. Bound biotinylated protein was eluted by incubation of the beads with 50 μl of 5% β-mercaptoethanol in PBS for 30 min in a 37 °C water bath. The elution was repeated two more times to maximize protein recovery. Approximately 20 μg of protein was eluted by this method. For LC/MS analysis, 4 μg of protein was digested using an in-gel tryptic digestion kit (Pierce) and analyzed by University of California Davis proteomic core facility.

HMGB1 and sRAGE—U937 cells (1.2×10^9) were chilled at 4 °C for 6 h, sedimented by centrifugation, and lysed in cold lysis buffer (1% Triton X-100, 20 mM Tris, pH 8, 150 mM NaCl) supplemented with protease inhibitors (Sigma). The cell lysate was centrifuged at $14,000 \times g$ for 20 min, and the supernatant was diluted with 50 mM Tris (pH 8.1) to achieve a final NaCl concentration of 60 mM. The diluted lysate was applied to a DEAE HiTrap column (2×1 ml, GE Healthcare). HMGB1 eluted between 150 to 240 mM salt at pH 8.1. The pooled fractions were applied to a 1.3-ml UNO-Q column (Bio-Rad) after diluting the NaCl concentration to 80 mM. HMGB1 eluted between 200 to 325 mM salt at pH 8.1. The partially purified HMGB1 was then applied to a 1-ml heparin-Sepharose column, and HMGB1 was eluted between 550 mM to 600 mM salt at pH 7.1. In the last step of purification, pooled heparin fractions was concentrated and resolved by a G2000SW gel permeation column (Tosoh). Approximately 50 μg of highly pure HMGB1 (at least > 95% pure as judged by silver staining of PAGE gels after analysis of 200 ng of material) was obtained.

In experiments employing mutants of HMGB1, recombinant protein was generated in *Escherichia coli*. The complete open reading frame of human HMGB1 (Open Biosystems) was cloned into pET45b (Novagen) using the *PshA* I site. Expression was carried out in Origami-B cells (Novagen) carrying the pGro7 (Takara) plasmid expressing chaperonin proteins GroEL and GroES of *E. coli*. Transformed cells were grown in LB medium supplemented with 12.5 μg/ml tetracycline, 15 μg/ml kanamycin, 35 μg/ml chloramphenicol, and 50 μg/ml carbenicillin at 37 °C. When the absorbance at 600 nm reached 0.4–0.7, isopropyl β-D-thiogalactopyranoside (0.15 mM) and L-arabinose (1 mg/ml) were added to induce the expression of HMGB1 and chaperonin proteins, respectively. The cells were allowed to shake overnight at 22 °C. Purification was carried out using a Ni-Sepharose 6 fast flow column, followed by gel permeation chromatography with HiLoad 16/60 Superdex 75 and anion exchange chromatography with MonoQ 5/50 (GE Healthcare). Mutagenesis was performed using a QuikChange site-directed mutagenesis kit (Agilent).

The extracellular domain (Ala-23–Glu-326) of RAGE was cloned into pET45b using PshA I site. Expression was carried out in the same way as described for HMGB1. Purification was performed by using a Ni-Sepharose 6 fast flow column followed by gel filtration chromatography with Superdex 200 10/300.

Biotinylation of HMGB1 and sRAGE—HMGB1 or sRAGE was diluted in 3 ml of PBS and was loaded onto a 200-μl heparin-Sepharose column. Sulfo-NHS-LC-biotin in PBS (500 μl of a 1 mM solution, pH 8) was then applied to the column, and biotinylation was allowed to proceed for 30 min at room temperature. The reaction was stopped by applying 600 μl of PBS containing 100 mM glycine, pH 7. After washing the column with 1 ml of 20 mM HEPES buffer (pH 7.1) containing 150 mM NaCl, the column was eluted sequentially with 600 mM NaCl and 1 M NaCl in 20 mM HEPES buffer (800 μl). Protein eluted by 1 M NaCl was used for all binding experiments.

HMGB1 and sRAGE Binding to Immobilized Heparin and Heparan Sulfate—Porcine mucosal heparin (SPL Scientific Protein Laboratories) and bovine kidney heparan sulfate (Sigma) were immobilized (0.1 ml of 10 μg/ml) on 96-well heparin binding plates (BD Biosciences) according to the manufacturer's instructions. Plates were blocked with 5% BSA in PBS and incubated with various concentrations of biotinylated HMGB1 or sRAGE. Bound ligand was quantitated with streptavidin-HRP (Jackson Immunology) followed by the addition of HRP substrate (Thermo Scientific).

HMGB1 and sRAGE Binding to CHO Cells—Wild-type CHO-K1 cells or heparan sulfate-deficient mutants pgsD, pgsE, and pgsF (5×10^5 cells) (13) were incubated with biotinylated HMGB1 (1 μg/ml) or sRAGE (2 μg/ml) in 100 μl of PBS for 1 h at 4 °C. After rinsing, the cells were stained with streptavidin-phycoerythrin (eBioscience) at a dilution of 1:1000 for 15 min and analyzed by flow cytometry. In some experiments, cells were treated with heparin lyases I (2 milliunits/ml), II (2 milliunits/ml), and III (5 milliunits/ml) for 15 min at room temperature prior to binding experiments. In some experiments, heparin, 2-*O*-desulfo-heparin and 6-*O*-desulfo-heparin and *N*-desulfo/re-*N*-acetylated heparin (Neoparin, Inc.) were included (10^{-11} to 10^{-5} mol/liter). The geometric means of binding histograms obtained in the presence of heparin were

TABLE 1
Extracellular heparin-binding proteins identified by mass spectrometry

NCBI Protein ID	Protein	Subcellular location[a]	Heparin binding[b]	Peptide coverage		
				1st	2nd	3rd
					%	
P23284	Cyclophilin B	Ex/Cp	Yes	62	66	70
P09429	High mobility group protein B1	Nu/Cp/Ex	Yes	60	34	55
P26038	Moesin	Cp/Ex	Yes	48	56	57
P04075	Fructose-bisphosphate aldolase A	Cp/Ex	Yes	58	22	54
Q06830	Peroxiredoxin-1	Cp/Ex	NA	24	45	50
P05455	Lupus La protein	Nu/Ex	NA	31	17	45
P51858	Hepatoma-derived growth factor	Ex/Nu	Yes	19	46	19
P19338	Nucleolin	Nu/Ex	Yes	31	26	22
P08567	Pleckstrin	Cp	NA	17	30	15
Q13765	Nascent polypeptide-associated complex subunit α	Cp	NA	27	26	14
P06748	Nucleophosmin	Nu/Ex	Yes	31	9	17
P30533	α-2-Macroglobulin receptor-associated protein	Ex	Yes	23	12	18
P62937	Cyclophilin A	Ex/Cp	Yes	9	13	43
O60506	Heterogeneous nuclear ribonucleoprotein Q	Nu	NA	33	7	9
P14866	Heterogeneous nuclear ribonucleoprotein L	Nu	NA	10	6	22
P08238	Heat shock protein HSP 90-β	Cp/Ex	Yes	9	16	12
Q14444	Caprin-1	Cp	NA	10	6	10
O43390	Heterogeneous nuclear ribonucleoprotein R	Nu	NA	9	4	10
Q12906	Interleukin enhancer-binding factor 3	Nu/Cp	NA	11	6	5
P07900	Heat shock protein HSP 90-α	Cp/Ex	Yes	6	4	10
P11021	78-kDa glucose-regulated protein	Cp/Ex	Yes	8	6	5

[a] Nu, Nuclear; Cp, cytoplasmic; Ex, extracellular.
[b] NA, data not available.

normalized to the one obtained in the absence of heparin and expressed as a percentage of maximum binding. The inhibition curve was fitted to one site competition, and IC_{50} values were calculated in Prism.

Endothelial Cell Sprouting Assay—Isolation of murine brain and lung microvascular endothelial cells and a sprouting assay using rat tail type I collagen gel (BD Biosciences) were performed essentially as described (14). Highly purified U937 cell endogenous HMGB1 or FGF2 (Shenandoah Biotechnology) was diluted in DMEM to the desired concentration. The net length of endothelial sprouts per (100×) microscopic field was measured after 24 h. Data were normalized to the response of unstimulated cells and expressed as fold stimulation.

Immunoblotting—Human cardiac microvascular endothelial cells (HMVEC-c) cells (Lonza, cc-7030) were serum-starved in DMEM for 5 h prior to treatment with U937-derived HMGB1. In some experiments, HMVEC-c were incubated with a mixture of heparin lyases I (2 milliunits/ml), II (2 milliunits/ml), and III (5 milliunits/ml), or with 10 μg/ml protamine (Sigma), or with 10 μg/ml blocking antibody to RAGE (R&D Systems) in serum-free DMEM at 37 °C for 15 min. Cells were then stimulated with 50 to 2500 ng/ml HMGB1 at 37 °C for 10 min. Cells were lysed in radioimmune precipitation assay buffer (Cell Signaling) containing protease and phosphatase inhibitors (Pierce). Samples (10 μg) were resolved on 4–12% Bis-Tris NuPage gel and blotted onto polyvinylidene difluoride membrane. After incubation with primary and secondary antibodies to Erk1/2, phospho-Erk1/2, and phospho-p38 (Cell Signaling), reactive bands were visualized by West Pico chemiluminescent substrate (Pierce).

Proximity Ligation Assay—Proximity ligation was measured using a mouse monoclonal antibody (10E4, US Biological) to heparan sulfate and an affinity-purified rabbit polyclonal antibody to human RAGE extracellular domain (Millipore), diluted to 1 μg/ml, and processed as described previously (15).

RESULTS

Identification of Monocyte Surface-expressed Heparin-binding Proteins—A four-step proteomic approach was designed to discover heparin-binding proteins present on cells. U937 human monocytic cells were biotinylated with the impermeant reagent, Sulfo-NHS-SS-Biotin. Biotinylated proteins were then purified by heparin-Sepharose and streptavidin affinity chromatography. Analysis by liquid chromatography/mass spectrometry yielded 21 heparin-binding proteins, many with high sequence coverage (Table 1). Twelve of the identified proteins have been shown previously to bind to heparin. Interestingly, nine proteins are classified as nuclear and 11 are classified as cytoplasmic proteins. We were surprised at first that so many of the tagged proteins were cytoplasmic or nuclear residents. Contamination by cell lysis during the biotinylation step seemed unlikely because more abundant heparin-binding nuclear proteins, such as histones, were not identified in any of the preparations. An in-depth literature search revealed that many of the identified nuclear proteins can be secreted, including HMGB1, lupus La protein, hepatoma-derived growth factor, nucleolin, and nucleophosmin (16–19). None of the three heterogeneous nuclear ribonucleoproteins (hnRNPs Q, L, and R) have been shown to be expressed extracellularly, but surface expression is likely because a related protein hnRNP U has been observed at the cell surface (20). In subsequent studies, we focused on the heparin-binding properties of HMGB1 as a paradigm for future studies of the other proteins discovered in this proteomic screen.

Binding of HMGB1 to CHO Cells Depends on Heparan Sulfate—HMGB1 was identified originally as a DNA-binding protein, and its capacity to bind heparin was exploited for its purification (21). HMGB1 also can bind heparan sulfate proteoglycans, but the biological significance of this interaction has not been explored (22). Incubation of biotinylated HMGB1 with immobilized heparin or bovine kidney heparan sulfate

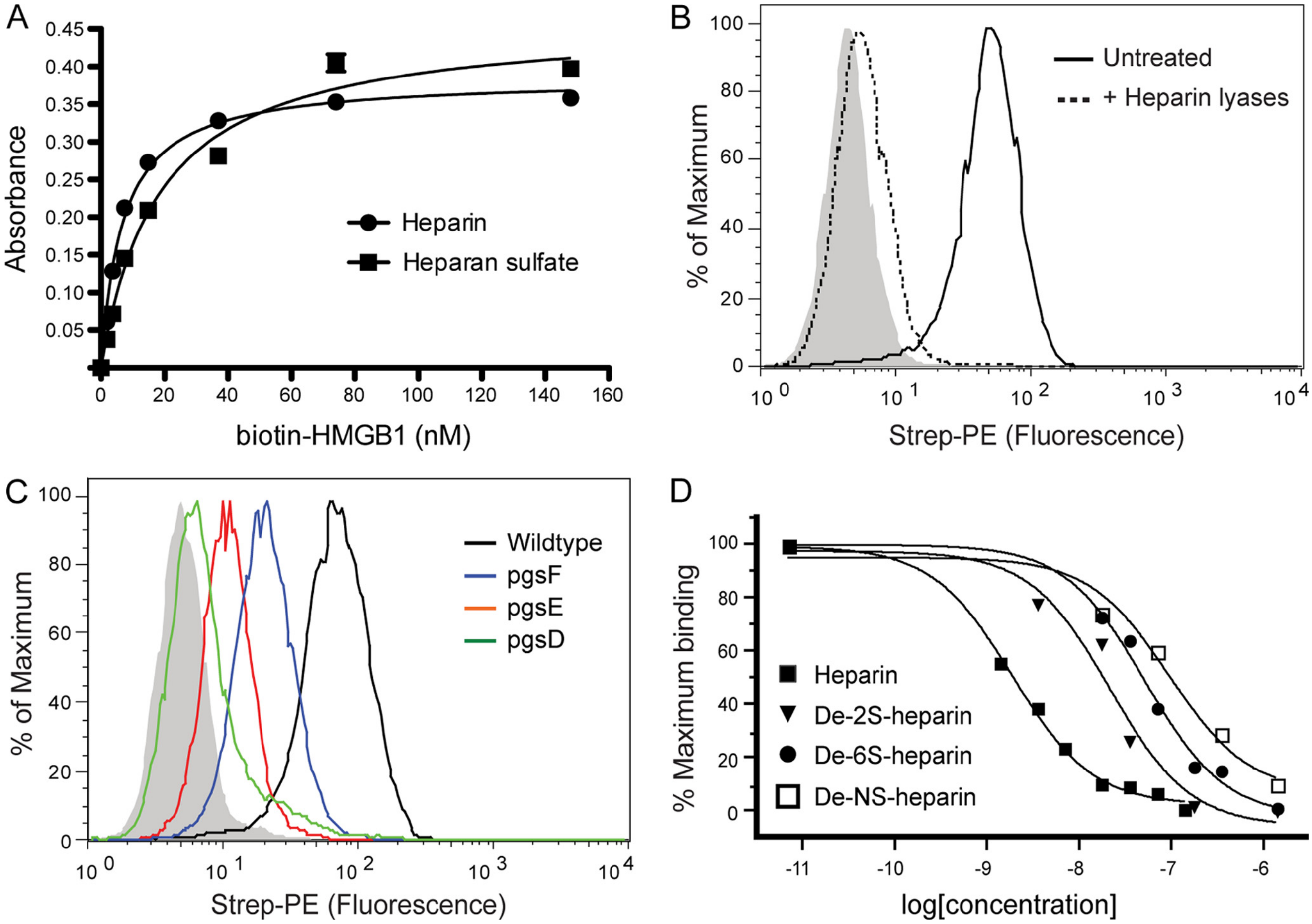

FIGURE 1. **Binding of HMGB1 to CHO cells depends on heparan sulfate.** *A*, binding of biotinylated recombinant HMGB1 to immobilized heparin (*circles*) and heparan sulfate (*squares*) was measured. *B*, binding of biotinylated HMGB1 (1 μg/ml) to CHO-K1 cells was measured by flow cytometry with or without heparin lyase pretreatment. The control sample was incubated only with streptavidin-phycoerythrin (*Strep-PE*) and is shown as a *filled gray* histogram. *C*, binding to wild-type CHO-K1 is shown in *black*, to 2-*O*-sulfation-deficient mutant pgsF in *blue*, to *N*-sulfation-deficient mutant pgsE in *red*, and to heparan sulfate-deficient mutant pgsD in *green*. *D*, HMGB1 binding was performed by flow cytometry in the presence of 10^{-11} to 10^{-6} M heparin or chemically desulfated heparins. Shown are the relative fluorescence units normalized to maximum binding.

yielded K_d values of 6.8 ± 0.4 nM and 18.4 ± 2 nM for heparin and heparan sulfate, respectively (Fig. 1*A*).

Heparin lyase treatment of CHO cells showed that binding of biotinylated recombinant HMGB1 strictly depends on heparan sulfate and not other glycosaminoglycans (Fig. 1*B*). CHO pgsD-677 cells, which lack heparan sulfate but make elevated amounts of chondroitin/dermatan sulfate (supplemental Fig. S1*A*), also fail to bind HMGB1 (Fig. 1*C*, relative fluorescence units (RFU) = 2 *versus* 64 in mutant and wild-type cells, respectively). Binding decreased in pgsE-606 (RFU = 8) and in pgsF-17 (RFU = 17) cells that lack glucosamine *N*-sulfotransferase and uronyl 2-*O*-sulfotransferase activities, respectively (Fig. 1*C*). Heparin, a highly sulfated form of heparan sulfate, blocked binding to wild-type cells with an IC_{50} of 1.8 ± 0.2 nM (Fig. 1*D*). Competition studies using various desulfated versions of heparin confirmed that loss of sulfate groups from any position significantly reduced the capacity of heparin to block binding (Fig. 1*D*, IC_{50} values = 21 ± 6, 49 ± 8, and 90 ± 30 nM for 2-*O*-desulfo-, 6-*O*-desulfo, and *N*-desulfo heparins). The dramatic reduction of potency when *N*-sulfate groups were removed is consistent with the equally dramatic loss of binding to pgsE cells. The combined genetic and competition studies suggests the order of importance of sulfate groups in binding of HMGB1 to heparin/heparan sulfate is *N*-sulfation > 6-*O*-sulfation > 2-*O*-sulfation. This pattern differs significantly from the behavior of FGF2, which depends more on 2-*O*-sulfation than *N*-sulfation in this assay (supplemental Fig. S1*B*).

Location of Heparan Sulfate-binding Site of HMGB1—Most ligands bind to heparin/heparan sulfate by way of electrostatic interactions of the negatively charged sulfate groups and uronic acids in the chains with positively charged lysine and arginine residues in the ligand. HMGB1 contains a large number of basic residues, 43 lysines and 8 arginines, which account for 24% of the amino acids (Fig. 2*A* and supplemental Fig. S2). To determine the relevant lysine residues for binding, we used a mapping strategy that combines biotinylation, heparin affinity chromatography, and mass spectrometry. Briefly, HMGB1 was bound to heparin-Sepharose, biotinylated *in situ*, and then eluted stepwise with a salt gradient. Unmodified HMGB1 eluted as a sharp peak centered ~555 mM NaCl. After biotinylation, the majority of the HMGB1 eluted at significantly lower salt concentration (supplemental Fig. S3), suggesting that lysine residues relevant to binding had been modified. In theory, molecules that elute with lower salt should contain more biotiny-

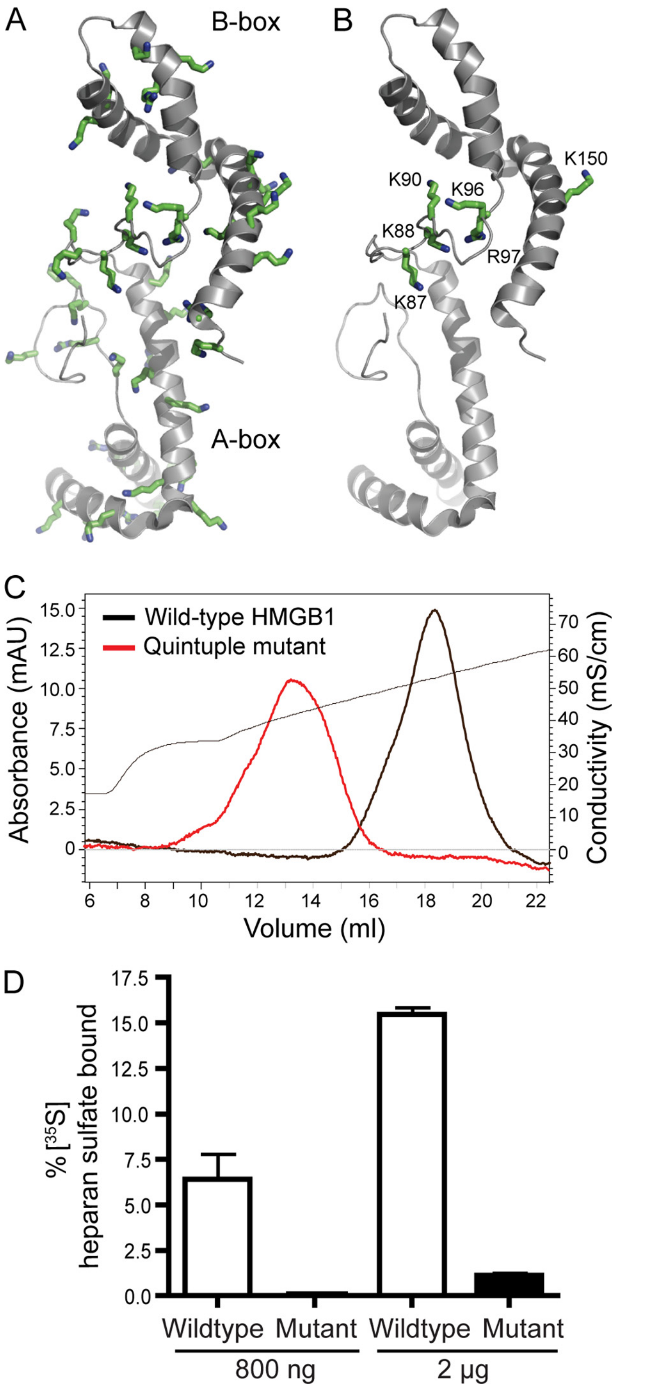

FIGURE 2. **A cluster of basic residues located at the loop region of HMGB1 contributes to heparan sulfate binding.** *A*, schematic representation of a solution structure of HMGB1 (Protein Data Bank code 2YRQ). The HMGB1 A-box is shown in *light gray*, and the B-box is shown in *dark gray*. The side chains of all basic residues are shown as *green sticks*. *B*, basic residues that contribute to heparan sulfate binding as determined by site-directed mutagenesis. *C*, heparin-Sepharose chromatography of wild-type HMGB1 and quintuple mutant K87A/K88A/K96A/R97A/K150A. The conductivity trace is shown as a *thin black line*. *D*, binding of wild-type HMGB1 and K87A/K88A/K96A/R97A/K150A mutant (800 ng or 2 μg) to ^{35}S-labeled endothelial heparan sulfate as determined by filter assay ($n = 3$, *error bar* represents S.E.). *mAU*, milliabsorbance units.

lated lysines residues involved in binding than molecules that bind at higher salt, whereas the latter should contain biotinylated lysines dispensable for binding. Assisted by mass spectrometry, we found that most lysine residues located within the major box domains (A-box domain, residues 13–79, and B-box, residues 99–163) were biotinylated in HMGB1 eluting in the high salt fractions 14–15, suggesting they were not essential for heparin binding (supplemental Table S1). In contrast, none of the lysine residues within the long loop region that connects the A- and B-boxes (residues 79–99) were biotinylated in high salt fractions, whereas many of them (Lys-82, Lys-87, Lys-88, and Lys-90) were biotinylated in lower salt fractions.

TABLE 2
Salt concentration for elution of HMGB1 mutants from heparin-Sepharose

Mutant	Peak NaCl
Wild-type HMGB1	555 mM
R10A/K12A	545 mM
K68A/R70A	555 mM
K82A	555 mM
K87A/K88A	500 mM
K90A	515 mM
K96A/R97A	500 mM
R110A/K112A	550 mM
K141A	550 mM
K152A/K154A	545 mM
R163A	550 mM
167stop	550 mM
K87A/K88A/K96A/R97A	445 mM
K87A/K88A/K96A/R97A/K150A	410 mM
K87A/K88A/K96A/R97A/K8A	435 mM
K87A/K88A/K96A/R97A/K90A	Not soluble
K87A/K88A/K96A/R97A/K90Q	425 mM
K87A/K88A/K96A/R97A/K86Q	445 mM

Based on this information and phylogenetic comparisons indicating conservation of a subset of lysine and arginine residues (supplemental Fig. S2), we selected a number of residues for mutagenesis (Table 2). Most of the selected mutations did not alter the elution of HMGB1 from heparin-Sepharose, except those located within the loop region (K87A–K88A, K90A, K96A–R97A). Various combinations of mutations showed that residues Lys-87, Lys-88, Lys-96, and Lys-97 from the loop region and Lys-150 from the B-box were most relevant to binding (Table 2 and Fig. 2*B*). The quintuple mutant bound to heparin less avidly, eluting at 410 mM NaCl (Fig. 2*C*). The quintuple mutant at physiological salt concentration essentially lost the capacity to bind [^{35}S]heparan sulfate prepared from endothelial cells (Fig. 2*D*), which presumably reflects the lower overall sulfation of heparan sulfate compared with heparin.

HMGB1-induced Sprouting Is Substantially Reduced in Ndst1-deficient Endothelial Cells—To determine whether the interaction of HMGB1 with heparan sulfate affected its biological activity, we derived primary microvascular endothelial cells from *Ndst1*$^{f/f}$*Tie2Cre*$^{+}$ mice, which, similar to CHO pgsE cells, are deficient in glucosaminyl *N*-deacetylase-*N*-sulfotransferase-1 (15). Binding of HMGB1 to mutant endothelial cells was reduced to 5% of wild-type (Fig. 3*A*), which agrees well with reduced HMGB1 binding to CHO pgsE cells (Fig. 1*B*). Sprouting of primary endothelial cells on type I collagen was stimulated by HMGB1 as much as 4.3-fold above untreated control cells reaching a maximum at 10 ng/ml (Fig. 3*B*). On a molar basis, HMGB1 was ~60% as potent as FGF2 in inducing endothelial sprouting. Sprouting of Ndst1-deficient endothelial cells was greatly reduced when challenged with either HMGB1 or FGF2 (Fig. 3*B*), demonstrating the importance of heparan sulfate.

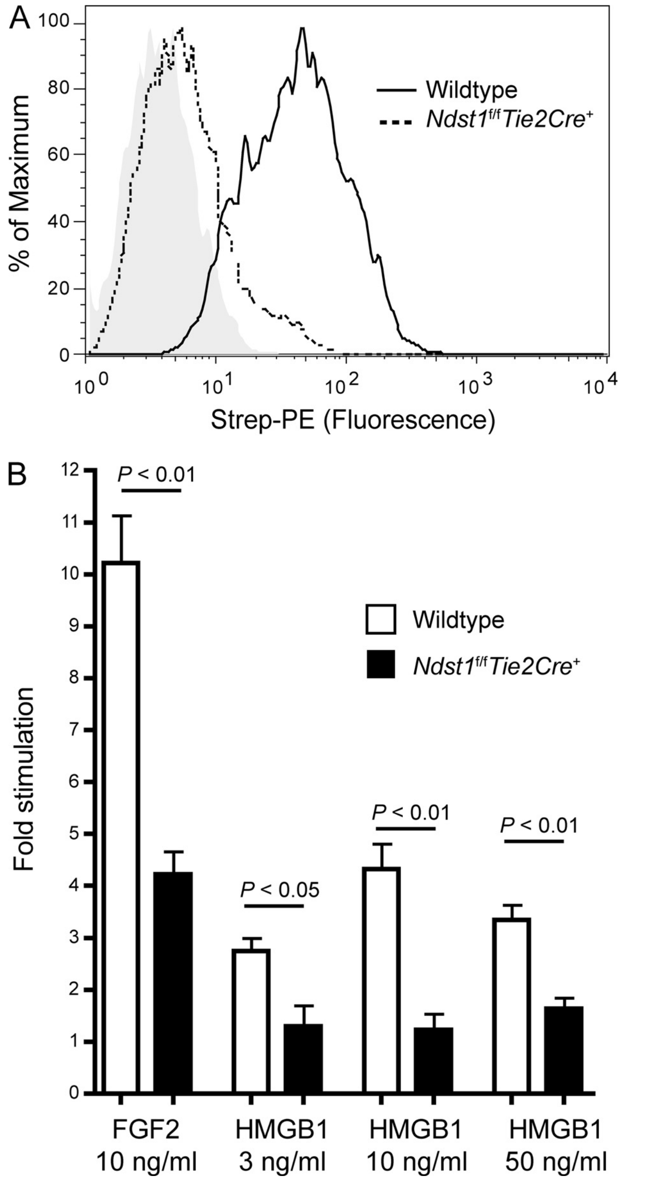

FIGURE 3. **HMGB1-induced sprouting in Ndst1-deficient endothelial cells.** *A*, binding of biotinylated HMGB1 (2 μg/ml) to wild-type or Ndst1-deficient mouse microvascular endothelial cells was measured by flow cytometry. *B*, sprouting of mutant and wild-type mouse endothelial cells on collagen in response to HMGB1 after 24 h treatment. Data are mean values ± S.E. for net length of endothelial sprouts per 100× microscopic field, normalized to the response of unstimulated wild-type cells (n = 4). *Strep-PE*, streptavidin-phycoerythrin.

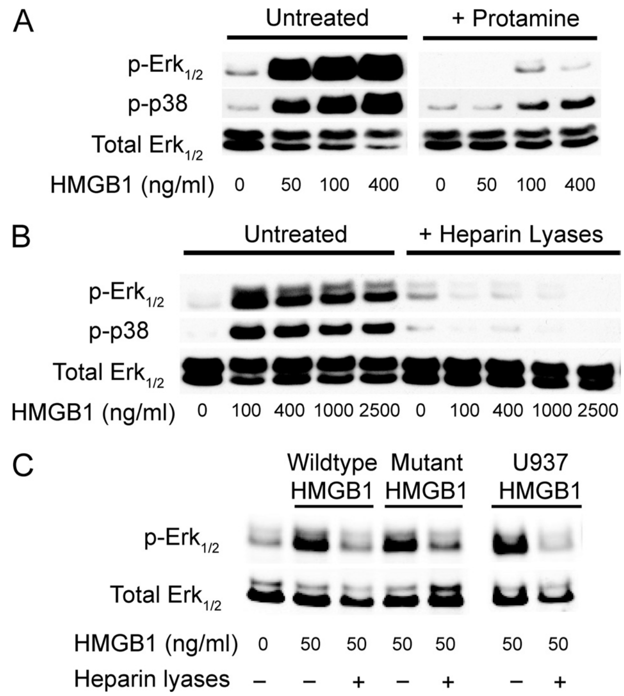

FIGURE 4. **HMGB1-induced** Erk1/2 **and p38 phosphorylation.** *A*, immunoblot analysis of Erk1/2 and p38 phosphorylation in HMVEC-c after stimulation with U937-derived HMGB1. HMVEC-c were preincubated with or without 1 μM protamine and then treated with 50 to 400 ng/ml of HMGB1 for 10 min. *B*, HMVEC-c were pretreated with or without heparan lyases I, II, and III for 15 min and then stimulated with 100 to 2500 ng/ml of HMGB1. All blots are representative of at least three similar experiments. *C*, immunoblot analysis of Erk1/2 phosphorylation in HMVEC-c after stimulation with 50 ng/ml of *E. coli* expressed wild-type HMGB1, K87A/K88A/K96A/R97A/K150A mutant or U937-derived HMGB1.

Stimulation of primary HMVEC-c with HMGB1 for 10 min resulted in phosphorylation of both Erk1/2 and p38 (Fig. 4*A*). Protamine, which is used to neutralize therapeutic heparin, or brief treatment with heparin lyases blocked phosphorylation of Erk1/2 and p38 (Fig. 4, *A* and *B*). Remarkably, heparin lyase-treated cells remained unresponsive to HMGB1 even at concentrations as high as 2500 ng/ml (Fig. 4*B*). This finding indicates that loss of heparan sulfate cannot be overcome by merely increasing the ligand concentration, which differs from the behavior of other heparin-dependent growth factors such as FGF2 (14). Attempts to measure signaling responses in murine endothelial cells were met with very high background, preventing analysis of heparan sulfate-deficient cells.

We next examined whether the quintuple mutant of HMGB1 was able to induce phosphorylation of Erk1/2. To our surprise, despite complete loss of heparan sulfate binding (Fig. 2*D*), mutant HMGB1 induced Erk1/2 phosphorylation as well as the control (Fig. 4*C*). Nevertheless, induction of Erk1/2 phosphorylation depended on cell surface heparan sulfate because heparin lyase treatment abolished phosphorylation (Fig. 4*C*). This finding indicated that heparan sulfate must be essential for the function of certain cell surface receptors critical for HMGB1 signaling.

Heparan Sulfate Interacts with RAGE—The cytokine function of extracellular HMGB1 is mediated primarily through RAGE. Like HMGB1, sRAGE binds to heparin and heparan sulfate with relatively high affinity (4.8 ± 0.4 nM and 28 ± 2.4 nM for heparin and heparan sulfate, respectively) (Fig. 5*A*, compare with Fig. 1*A*). sRAGE also binds to CHO cells in a heparan sulfate-dependent manner based on heparin lyase treatment (RFU = 3 *versus* 43, Fig. 5*B*) and studies of pgsD cells (RFU = 2.5 *versus* 43, Fig. 5*C*). Binding to pgsE cells was reduced to 33% (RFU = 14 *versus* 43, Fig. 5*C*), suggesting that *N*-sulfation was important for binding. Interestingly, binding was only very slightly reduced in pgsF cells (RFU = 35 *versus* 43, Fig. 5*C*), suggesting that 2-*O*-sulfation was dispensable. Heparin blocked binding to wild-type cells with an IC_{50} of 3.2 ± 1.1 nM. 2-*O*-desulfo- and 6-*O*-desulfo-heparin competed almost as well as unmodified heparin (IC_{50} = 4.1 ± 0.9 and 4.1 ± 1.4 nM, respectively), which suggests that sulfation at these positions

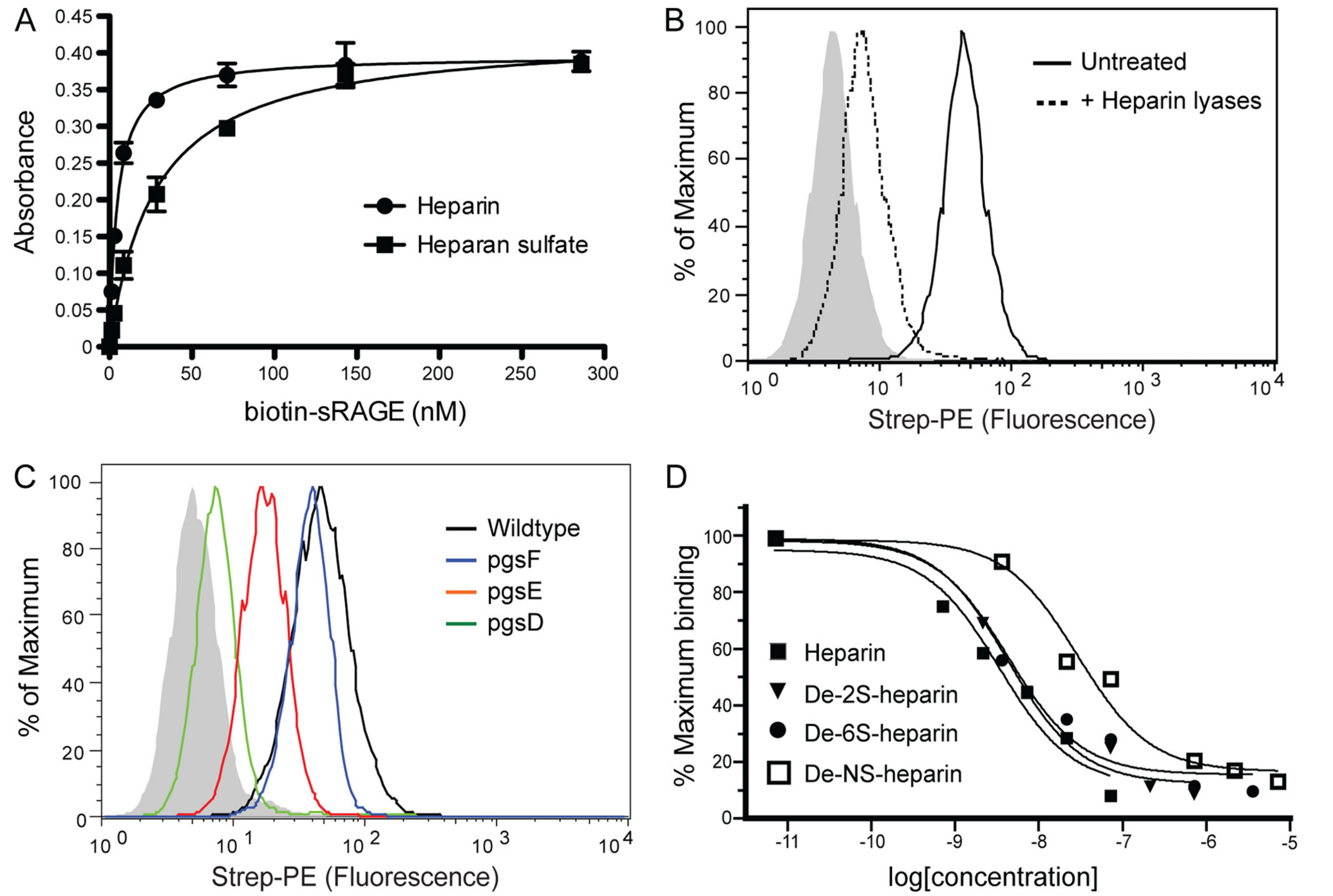

FIGURE 5. **RAGE interacts with heparan sulfate.** *A*, binding of biotinylated sRAGE to immobilized heparin (*circles*) and heparan sulfate (*squares*) was measured. *B*, binding of biotinylated sRAGE (2 μg/ml) to wild-type CHO-K1 cells was measured by flow cytometry with or without heparin lyase pretreatment. *C*, binding of biotinylated sRAGE to various CHO mutants. *D*, heparin and various desulfated heparins compete for sRAGE binding to CHO cells. *Strep-PE*, streptavidin-phycoerythrin.

was not required for sRAGE binding (Fig. 5*D*). In contrast, *N*-desulfo-heparin competed poorly compared with heparin ($IC_{50} = 28 \pm 8.1$ nM; Fig. 5*D*). Thus, both RAGE and HMGB1 critically depend on *N*-sulfation for binding to heparan sulfate.

RAGE is a functional receptor for HMGB1 on HMVEC-c because a blocking antibody totally abolished the phosphorylation of Erk1/2 and p38 (Fig. 6*A*). We predicted that RAGE and heparan sulfate might form a complex at the cell surface. Using two antibodies, one against heparan sulfate and the other against RAGE, we showed by proximity ligation that complexes exist on the surface of endothelial cells. Interesting, the RAGE/heparan sulfate interaction was readily detected in the absence of HMGB1 (Fig. 6*B*), suggesting that there were preformed complexes of heparan sulfate and RAGE at endothelial surface. A time-dependent increase of association occurred after stimulation with HMGB1, increasing by 35% at 5 min (Fig. 6*B*), possibly as a result of receptor complex stabilization upon ligand binding.

DISCUSSION

In this study, we show that cell surface biotinylation coupled with heparin affinity chromatography tags many traditionally nuclear and cytoplasmic proteins. Although lysis of some cells could render these proteins susceptible to biotinylation, many other abundant heparin-binding proteins such as histones and various transcription factors, RNA binding proteins, and proteins involved in DNA replication were not detected. Other studies have shown that several of the tagged proteins are secreted via non-conventional pathways or during necrosis (17). Regardless of the mechanism, the release of nuclear and cytoplasmic proteins represents a danger signal that tissue damage has occurred. That so many of these proteins bind to heparin suggested that their extracellular activities might depend on cell surface heparan sulfate, which unlike heparin is expressed ubiquitously by virtually all animal cells. Indeed, among the identified proteins, cyclophilin A (23), cyclophilin B (24), and hepatoma-derived growth factor (25) have been shown to interact with heparan sulfate and cause a cellular response. Our attention was drawn to HMGB1 because it consistently showed very high peptide coverage in three proteomic screens, it is one of the major DAMPs released by necrotic cells during tissue injury, and it induces angiogenic and inflammatory responses in endothelial cells. We showed genetically and biochemically that HMGB1 is indeed a heparan sulfate dependent signaling factor, but to our surprise, the requirement for heparan sulfate is manifested at the level of the receptor RAGE rather than HMGB1.

Three other proteins identified in the screen belong to the heat shock protein (HSP) family (Table 1). Binding between

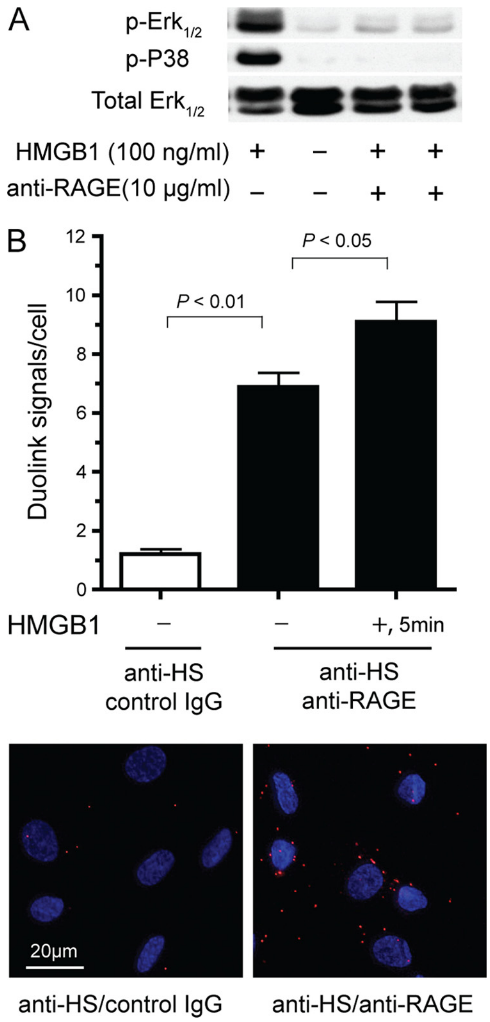

FIGURE 6. **RAGE-dependent signaling.** *A*, immunoblot analysis of Erk1/2 and p38 phosphorylation in HMVEC-c after stimulation with HMGB1. Some wells were preincubated with a blocking antibody (10 μg/ml) to RAGE for 20 min prior to stimulation. *B*, interaction between endogenous RAGE and heparan sulfate at the cell surface as measured by a proximity ligation assay. HMVEC-c cells were either unstimulated or stimulated with 100 ng/ml HMGB1 for 5 min, followed by fixation and incubation with antibodies to heparan sulfate, the extracellular domain of RAGE, and proximity ligation assay reagents. Each *red dot* indicates an interaction between heparan sulfate and RAGE. Nuclei are shown in *blue*. The data are presented as *red dots* (duolink signals) per cell. As a negative control, cells were incubated with anti-heparan sulfate antibody and nonspecific rabbit IgG. *Error bars* represent S.E. (n = 4 separate experiments). Representative images of unstimulated samples were shown in the *lower panel*.

HSPs and heparin has been documented as well, but whether the interaction is physiologically relevant has not been studied (26). Similar to HMGB1, HSPs are DAMPs released from necrotic cells during tissue injury and can trigger inflammatory responses (17, 27). This raises the interesting possibility that heparan sulfate, by interacting with multiple DAMPs, might serve as a central coreceptor that actuates the inflammatory response in injured tissue.

The interaction of heparan sulfate with FGF2-FGFR has become a paradigm for the action of heparan sulfate as a coreceptor (28, 29). However, the dependence of HMGB1 activity on heparan sulfate differs in several ways from the interaction of heparan sulfate with FGF2. First, *N*-sulfation plays a more prominent role in mediating heparan sulfate binding to HMGB1 than to FGF2 (Fig. 1*C* and supplemental Fig. S1*B*). Although the sprouting response of Ndst1-deficient endothelial cells to HMGB1 is completely abolished, its response to FGF2, albeit substantially reduced, remained significant (4.2-fold over untreated cells, Fig. 3*B*). Second, the requirement of heparan sulfate for signal transduction can be overcome by increasing the concentration of FGF2 (14), whereas even a 50-fold excess of HMBG1 (2.5 μg/ml) failed to induce signal transduction in the absence of heparan sulfate (Fig. 4*B*). The complete dependence of HMGB1 on heparan sulfate coreceptors suggests a fundamental difference in the way that RAGE and FGF receptors function.

HMGB1 bears an exceptionally large number of basic residues (24% of total amino acids). Mutagenesis revealed that only six basic residues make significant contribution to heparan sulfate binding. Five of these residues, Lys-87, Lys-88, Lys-90, Lys-96, Arg-97, are located within the second half of a long loop region that connects the A-box and B-box domains. A single residue in the last helix of B-box, Lys-150, also contributes significantly to binding. Combined, these residues form a contiguous string of positive charges that lie nearly perpendicular to the long axis of the HMGB1 (Fig. 2*B*). Four of the six residues, Lys-87, Lys-90, Lys-96, and Arg-97, also contribute to DNA binding (30, 31). However, DNA binding requires at least four additional charged residues in the A-box and six in the B-box (32). Therefore, it appears that HMGB1 uses overlapping but distinct basic residues for heparan sulfate and DNA binding.

The quintuple mutant K87A/K88A/K96A/K97A/K150A of HMGB1 represents an ideal tool to study the physiological consequences of blunted HMGB1/heparan sulfate interactions. By analogy, the quintuple mutant is similar to the non-heparin binding form of VEGF, VEGF121, which is able to bind and stimulate VEGF receptors (15). Similarly, the quintuple mutant of HMGB1 signals independently of its capacity to bind heparan sulfate (Fig. 4*C*). However, genetic studies have shown that mutant animals expressing only VEGF121 do not survive due to misregulated angiogenesis (33). This phenomenon can be explained by failure of VEGF121 to establish the correct spatial localization, whereas the heparin binding forms of VEGF can interact with heparan sulfate in the extracellular matrix and form the proper gradients needed to guide angiogenesis. A similar scenario may be relevant to HMGB1. When HMGB1 is released by necrotic tissue after damage, it presumably binds to heparan sulfate in the matrix, which in turn restricts the cellular responses to the area of local damage. We can test this hypothesis by injection or transgenic expression of the quintuple mutant *in vivo*.

During the inflammatory response, chemokines and cytokines secreted by monocytes or macrophages act directly on endothelial cells, and many of them function in a heparan sulfate-dependent manner (34). Endothelial heparan sulfate has profound effects on chemokine presentation, oligomerization, and transcytosis (35, 36). Similarly, heparan sulfate serves as a critical co-receptor for the proangiogenic factors FGF and VEGF by interacting with both ligands and receptors (14, 15, 37–39). We can now add HMGB1 and RAGE to the growing list of inflammatory mediators and receptors that depend on cell surface heparan sulfate. Although we used only endothelial cells in our studies, the importance of heparan sulfate in RAGE signaling may extrapolate to other cell systems expressing RAGE and other ligands that signal through this receptor.

Acknowledgments—We thank Geetha Srikrishna and Hudson Freeze for helpful discussions and providing reagents.

REFERENCES

1. Lotze, M. T., and Tracey, K. J. (2005) *Nat. Rev. Immunol.* **5,** 331–342
2. Gardella, S., Andrei, C., Ferrera, D., Lotti, L. V., Torrisi, M. R., Bianchi, M. E., and Rubartelli, A. (2002) *EMBO Rep.* **3,** 995–1001
3. Kono, H., and Rock, K. L. (2008) *Nat. Rev. Immunol.* **8,** 279–289
4. Klune, J. R., Dhupar, R., Cardinal, J., Billiar, T. R., and Tsung, A. (2008) *Mol. Med.* **14,** 476–484
5. Rauvala, H., and Rouhiainen, A. (2011) *Biochim. Biophys. Acta* **1799,** 164–170
6. Fiuza, C., Bustin, M., Talwar, S., Tropea, M., Gerstenberger, E., Shelhamer, J. H., and Suffredini, A. F. (2003) *Blood* **101,** 2652–2660
7. Mitola, S., Belleri, M., Urbinati, C., Coltrini, D., Sparatore, B., Pedrazzi, M., Melloni, E., and Presta, M. (2006) *J. Immunol.* **176,** 12–15
8. Sims, G. P., Rowe, D. C., Rietdijk, S. T., Herbst, R., and Coyle, A. J. (2010) *Annu. Rev. Immunol.* **28,** 367–388
9. Yan, S. F., Ramasamy, R., and Schmidt, A. M. (2010) *Circ. Res.* **106,** 842–853
10. Basta, G. (2008) *Atherosclerosis* **196,** 9–21
11. Hudson, B. I., Kalea, A. Z., Del Mar Arriero, M., Harja, E., Boulanger, E., D'Agati, V., and Schmidt, A. M. (2008) *J. Biol. Chem.* **283,** 34457–34468
12. Ishihara, K., Tsutsumi, K., Kawane, S., Nakajima, M., and Kasaoka, T. (2003) *FEBS Lett.* **550,** 107–113
13. Zhang, L., Lawrence, R., Frazier, B. A., and Esko, J. D. (2006) *Methods Enzymol.* **416,** 205–221
14. Fuster, M. M., Wang, L., Castagnola, J., Sikora, L., Reddi, K., Lee, P. H., Radek, K. A., Schuksz, M., Bishop, J. R., Gallo, R. L., Sriramarao, P., and Esko, J. D. (2007) *J. Cell Biol.* **177,** 539–549
15. Xu, D., Fuster, M. M., Lawrence, R., and Esko, J. D. (2011) *J. Biol. Chem.* **286,** 737–745
16. Christian, S., Pilch, J., Akerman, M. E., Porkka, K., Laakkonen, P., and Ruoslahti, E. (2003) *J. Cell Biol.* **163,** 871–878
17. Harris, H. E., and Raucci, A. (2006) *EMBO Rep.* **7,** 774–778
18. McArthur, C., Wang, Y., Veno, P., Zhang, J., and Fiorella, R. (2002) *Arch Oral Biol.* **47,** 443–448
19. Brandt, R., Nawka, M., Kellermann, J., Salazar, R., Becher, D., and Krantz, S. (2004) *Biochim. Biophys. Acta* **1670,** 132–136
20. Jordan, P., Heid, H., Kinzel, V., and Kübler, D. (1994) *Biochemistry* **33,** 14696–14706
21. Rauvala, H., and Pihlaskari, R. (1987) *J. Biol. Chem.* **262,** 16625–16635
22. Salmivirta, M., Rauvala, H., Elenius, K., and Jalkanen, M. (1992) *Exp. Cell Res.* **200,** 444–451
23. Saphire, A. C., Bobardt, M. D., and Gallay, P. A. (1999) *EMBO J.* **18,** 6771–6785
24. Allain, F., Vanpouille, C., Carpentier, M., Slomianny, M. C., Durieux, S., and Spik, G. (2002) *Proc. Natl. Acad. Sci. U.S.A.* **99,** 2714–2719
25. Wang, C. H., Davamani, F., Sue, S. C., Lee, S. C., Wu, P. L., Tang, F. M., Shih, C., Huang, T. H., and Wu, W. G. (2011) *Biochem. J.* **433,** 127–138
26. Ménoret, A., and Bell, G. (2000) *J. Immunol. Methods* **237,** 119–130
27. Millar, D. G., Garza, K. M., Odermatt, B., Elford, A. R., Ono, N., Li, Z., and Ohashi, P. S. (2003) *Nat. Med.* **9,** 1469–1476
28. Yayon, A., Klagsbrun, M., Esko, J. D., Leder, P., and Ornitz, D. M. (1991) *Cell* **64,** 841–848
29. Rapraeger, A. C., Krufka, A., and Olwin, B. B. (1991) *Science* **252,** 1705–1708
30. Stros, M., and Muselíková, E. (2000) *J. Biol. Chem.* **275,** 35699–35707
31. Taudte, S., Xin, H., and Kallenbach, N. R. (2000) *Biochem. J.* **347,** 807–814
32. Stott, K., Tang, G. S., Lee, K. B., and Thomas, J. O. (2006) *J. Mol. Biol.* **360,** 90–104
33. Carmeliet, P., Ng, Y. S., Nuyens, D., Theilmeier, G., Brusselmans, K., Cornelissen, I., Ehler, E., Kakkar, V. V., Stalmans, I., Mattot, V., Perriard, J. C., Dewerchin, M., Flameng, W., Nagy, A., Lupu, F., Moons, L., Collen, D., D'Amore, P. A., and Shima, D. T. (1999) *Nat. Med.* **5,** 495–502
34. Handel, T. M., Johnson, Z., Crown, S. E., Lau, E. K., and Proudfoot, A. E. (2005) *Annu. Rev. Biochem.* **74,** 385–410
35. Wang, L., Fuster, M., Sriramarao, P., and Esko, J. D. (2005) *Nat. Immunol.* **6,** 902–910
36. Proudfoot, A. E., Handel, T. M., Johnson, Z., Lau, E. K., LiWang, P., Clark-Lewis, I., Borlat, F., Wells, T. N., and Kosco-Vilbois, M. H. (2003) *Proc. Natl. Acad. Sci. U.S.A.* **100,** 1885–1890
37. Pellegrini, L., Burke, D. F., von Delft, F., Mulloy, B., and Blundell, T. L. (2000) *Nature* **407,** 1029–1034
38. Schlessinger, J., Plotnikov, A. N., Ibrahimi, O. A., Eliseenkova, A. V., Yeh, B. K., Yayon, A., Linhardt, R. J., and Mohammadi, M. (2000) *Mol. Cell* **6,** 743–750
39. Jakobsson, L., Kreuger, J., Holmborn, K., Lundin, L., Eriksson, I., Kjellén, L., and Claesson-Welsh, L. (2006) *Dev. Cell* **10,** 625–634